Consortium for Small-Scale Modelling

Technical Report No. 9

Operational Implementation of the Multilayer Soil Model

July 2006

DOI: 10.5676/DWD_pub/nwv/cosmo-tr_9

Deutscher Wetterdienst

MeteoSwiss

Ufficio Generale Spazio Aereo e Meteorologia

ΕΘΝΙΚΗ ΜΕΤΕΩΡΟΛΟΓΙΚΗ ΥΠΗΡΕΣΙΑ

Instytucie Meteorogii i Gospodarki Wodnej

Administratia Nationala de Meteorologie

Agenzia Regionale per la Protezione Ambientale del Piemonte

Agenzia Regionale per la Protezione Ambientale dell' Emilia-Romagna: Servizio Idro Meteo

Centro Italiano Ricerche Aerospaziali

Amt für GeoInformationswesen der Bundeswehr

www.cosmo-model.org

Editor: Massimo Milelli, ARPA Piemonte
Printed at Deutscher Wetterdienst, P.O. Box 100465, 63004 Offenbach am Main

Operational Implementation of the Multilayer Soil Model

E. Heise, B. Ritter, R. Schrodin

DWD
Offenbach
Germany

Contents

1 Introduction, configuration of the multi-layer soil model

During the last years a new multi-layer version of the GME/LM soil model was developed (Schrodin and Heise, 2002; Heise et al., 2003) to replace the former operational 2-layer version. It became operational in GME on September 27, 2004, and in LM with the new extended model area LME on September 28, 2005. The aim of this report is to describe the present state of experience gained with the new soil model during the first years of (pre)operational use.
The main reason for increasing the number of layers was the need to take into account for freezing/melting processes in the soil, which in the 2-layer model are neglected. Because of the comparably thick uppermost layer in that version, freezing/melting effects would cause near surface temperatures to stick close to 0^oC for much too long periods in situations where in reality temperatures change around the freezing point with considerable amplitudes. But the omission of freezing/melting results in too large amplitudes of the near surface temperature in these situations. Therefore, a new version of the soil model was developed. It's main characteristic is a very high resolution in the uppermost layers of the soil. In order to avoid problems with prescribing the lower boundary condition for the thermal part, it was decided to extend the soil model to a depth, in which the annual variation of temperature is negligible. The solution

$$\delta = \Delta T_s e^{z/D} e^{i(\omega t + z/D)} \tag{1}$$

of the heat conduction equation (where δ is the temperature difference to a constant deep soil temperature, ΔT_s is the amplitude of a periodic variation of the soil surface temperature with frequency ω, D is the e-folding depth for the temperature wave, and z is the vertical coordinate, negative downward), shows the amplitude reduction of the surface temperature wave with increasing depth in the soil. For typical values of the e-folding depth of an annual temperature wave in the soil ($D \approx 2m$) an amplitude reduction to roughly 3 % of the surface value is achieved in a depth of 7 m. This led to the layer structure as given in Figure 1. In correspondence with the solution of the heat conduction equation, the layer thickness increases exponentially with depth. An additional layer with a temperature being constant in time is added below 7.29 m. Here the annual mean atmospheric near-surface temperature is prescribed as a boundary condition.

In contrast to the former two-layer version, identical layer structures are used in the thermal and the hydrologic parts, respectively. However, in contrast to the thermal part no straightforward solution for the lower boundary condition is available for the hydrologic part. Therefore, we tentatively follow a suggestion expressed in the context of the EU-project ELDAS (http://www.knmi.nl/samenw/eldas/) and prescribe a flux-boundary-condition in a depth of 2.43 m. In this depth we only consider the gravitational drainage of water and neglect any water transport due to vertical soil water gradients. In ELDAS a detailed verification has been performed of multi-annual quasi two-dimensional simulations using the multi-layer soil model. Here data from the Rhône-AGGregation Experiment (Boone et al., 2001) have been used partly as forcing data and partly as verification data. The verification concentrated on the annual courses of the snow budget and of the runoff production. The results led to some reformulation of aspects of the soil model.
The soil model is still strictly one-dimensional, i. e., all horizontal transports of water and energy in the soil are neglected. The effect of freezing/melting of soil water/ice is taken into account. The formulation accounts for the capability of the soil to retain a certain amount of liquid water at temperatures well below the freezing point. A single layer snow module complements the soil model.
For details of the soil model formulation the reader should refer to the extended documentation of the soil model (Doms et al., 2005).

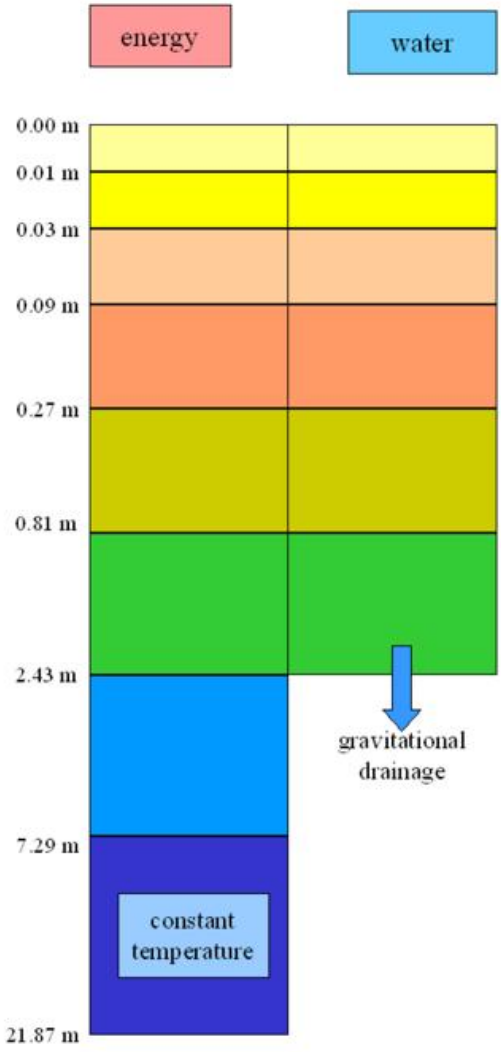

Figure 1:
Structure of the soil model

2 Operational use of the multi-layer soil model in the global model (GME) of DWD

Since September 2004 the multi-layer soil model is in operational use in the global model GME of the German Weather Service. A more than one year pre-operational run with GME preceded the operational introduction. During the operational use in GME some previously undetected problems were discovered, and a flux limiter was introduced.

2.1 Instability problems in connection with the interception store

In some cases an unfavourable interaction between the thin uppermost layer of the soil and the interception store was observed. As the interception store is not as important in the multi-layer model as in the former two layer model which used a thickness of the first layer of 0.1 m, the interception store was deactivated by setting it's maximum value to 10^{-6} m. The code related to the interception store was retained in order to allow for a later reuse of the interception store formulation.

2.2 Negative near surface temperature bias in the presence of snow, implementation of a prognostic treatment of snow density

In March 2005 excessive low temperatures were simulated over an old snow pack in southern Germany. The problem was traced back to the prescribed low density of the snow, which did not depend on external influences. The low value of snow density results in a) low heat conduction through the snow, and in b) a comparably thick snow layer for a given value of snow water equivalent. Both effects result in a very effective isolation between the soil surface and the top of the snow layer, leading to a de facto decoupling between soil and atmosphere. In order to overcome this problem, a time-dependent formulation of snow density was tested and implemented in GME. This formulation combines an ageing function, which simulates the various processes involved in the complex metamorphosis of an existing snow pack in a very crude way, with a reduction of the mean snow density in situations of fresh snow fall. The new value $\rho_{snow,new}$ of snow density at the end of time-step Δt is given by

$$\rho_{snow,new} = \left\{ \rho_{snow,age} W_{snow,old} + \rho_{snow,fresh} RR_{snow} \frac{\Delta t}{\rho_w} \right\} / W_{norm} \tag{2}$$

Here $W_{snow,old}$ is the snow water equivalent at the beginning of time-step Δt, ρ_w is the density of water. The ageing is accounted for by

$$\rho_{snow,age} = \rho_{snow,max} + (\rho_{snow,old} - \rho_{snow,max}) e^{-C_{age} \Delta t / \tau_\rho}, \tag{3}$$

where $\rho_{snow,old}$ is the snow density at the beginning of time-step Δt, and

$$C_{age} = 0.2 + (0.4 - 0.2) \cdot \frac{T_{snow} - T_{min}}{T_0 - T_{min}} \tag{4}$$

T_0 is the freezing point and we use $T_{min} = 258.15$ K. The time constant is set to $\tau_\rho = 1d$. The density of fresh falling snow is parameterized by

$$\rho_{snow,fresh} = \rho_{s,f,min} + (\rho_{s,f,max} - \rho_{s,f,min}) \cdot \frac{T_{low} - T_{min}}{T_0 - T_{min}}, \tag{5}$$

where $\rho_{s,f,min} = 50\ kg/m^3$, $\rho_{s,f,max} = 150\ kg/m^3$, and T_{low} is the temperature in the lowest atmospheric level. Finally, RR_{snow} is the rate of snowfall, and $W_{norm} = W_{snow,old} + RR_{snow}\frac{\Delta t}{\rho_w}$. The whole range of snow densities is restricted to $\rho_{snow,min} = 50\ kg/m^3$ and $\rho_{snow,max} = 400\ kg/m^3$.

In connection with the implementation of a time dependent snow density the determination of the snow heat conductivity was changed to

$$\lambda_{snow} = \lambda_{ice} \left\{ \frac{\rho_{snow}}{\rho_{ice}} \right\}^{1.88}, \tag{6}$$

where $\lambda_{ice} = 2.22\ W/(mK)$ is the heat conductivity of ice.

These changes became operational in GME on December 7, 2005.

2.3 High-frequency small-amplitude waves in the surface temperature

There is a tendency of the multi-layer soil model to produce $2\Delta t$-waves of small amplitude in the soil surface temperature. Normally these waves are not harmful to the rest of the (atmospheric) model. But in one case the effect became a problem because of an unfavourable coupling with atmospheric temperatures at grid-points with very large values of the roughness length. The small wave in the surface temperature combined with a more or less constant atmospheric temperature resulted in an alternation between stable and unstable stratification. Because of the large roughness length this led to a large-amplitude $2\Delta t$-wave in the transfer coefficient which resulted in a large-amplitude $2\Delta t$-wave in the diagnosed gusts. The runs with the LME seem not to be prone to this problem as LME uses a different formulation of the surface layer processes. In GME since August 24, 2005, the roughness length is restricted to 50 % of the height of the lowest atmospheric main level in order to overcome this problem.

2.4 Unfavourable interaction with the snow analysis

During the test-phase of the multi-layer soil model in combination with the assimilation cycle of GME it happened that snow cover was analysed in grid-elements with a soil surface temperature above the freezing point. As the analysed snow has the priority over the first guess of the model (zero snow cover in these grid-elements), an adjustment of soil temperatures is necessary. This was done by reducing the soil surface temperature to $0^o C$. In order to avoid too strong vertical gradients of the soil temperature across the first layer, a correction was applied to all soil layers with the temperature increment at the surface being linearly reduced to zero in the depth of the main level of the climate layer. In some parts of the Himalayas this led to soil temperatures of $0\,K$ during summer. The reason was a perpetual insertion of a few mm of snow in each analysis step. During the forecast this snow melted very fast, and soil surface temperatures increased considerably. But the next snow cover analysis again produced snow, and the correction had to be applied again. In the upper soil layers the energy gain due to solar radiation compensated the artificial temperature reduction in the analysis step and prevented temperatures from decreasing too much. But in the lower soil layers there was no effect counteracting the continual reduction of temperature. Therefore, the correction had to be modified. Now it is applied only in those uppermost layers, which exhibit temperatures above the freezing point. This version is applied since the start of the operational use of the multi-layer soil model in GME.

2.5 Limitation of transfer coefficients to alleviate stability problems in the multi-layer soil model

The continuous evolution of atmospheric and soil state variables which occur in the real world is not always guaranteed in the context of an NWP model. Abrupt changes may be caused in data assimilation steps but also within the actual forecast, where abrupt changes in the forcing terms (e.g. solar radiative surface flux) may be introduced as a consequence of a numerical method (e.g. rather infrequent calls of the radiative transfer scheme). If the inertia of model and soil layers is sufficiently large compared to the magnitude of the disturbances, a new balanced state can be achieved within a limited number of forecast time steps. If, in contrast, the disturbance is large compared to the model inertia, overshooting reactions may occur, which can subsequently lead to numerical instability.

The current multi-layer soil model, which features a top layer thickness of 1 cm, is prone to such over-reactions, following significant instantaneous changes in variables like snow water content or near surface wind in the analysis step or abrupt changes in the solar forcing caused by large variations in cloud cover between radiation time steps.

2.5.1 Turbulent transfer coefficient limitation at the surface

The overshooting reaction can be alleviated in many situations through the introduction of a situation-dependent upper limit for the turbulent fluxes exchanged between atmosphere and soil. For this purpose the flux will, if possible, be constrained such that the temporal tendency of the uppermost soil layer, i.e. the one with the smallest thermal inertia, does not exceed a prescribed limit in a single model time step.

The temperature tendency for each soil layer follows from:

$$\rho_{soil} c_{soil} \frac{\partial T_{soil}}{\partial t} = -\frac{\partial G}{\partial z} \tag{7}$$

with a typical value of the soil heat capacity of

$$\rho_{soil} c_{soil} = 1.4 \cdot 10^6 \frac{J}{m^3 K} \tag{8}$$

In (7) T_{soil} represents the soil temperature, z the soil depth and G the soil heat flux, which at the upper boundary is replaced by the surface fluxes of radiation, sensible and latent heat flux. For simplicity we will ignore the contributions by internal sources and sinks like melting and freezing of soil water.

Postulating an upper limit for the temporal temperature increment $\Delta T_{soil,max}$, we may derive a threshold for the heat flux at the earths surface. In discretized form we obtain:

$$\left| \frac{G(0) - G(1)}{z(0) - z(1)} \right| \leq \rho_{soil} c_{soil} \frac{\Delta T_{soil,max}}{\Delta t} \tag{9}$$

where the depths z refer to the half levels of the soil model grid and may be replaced by the thickness of the first soil layer, which we will denote byΔz_{soil}.

The presence of snow on the ground may be incorporated in (9) through the addition of a component representing a potential heating and melting of the snow layer. Based on (9) we then obtain:

$$\begin{aligned} &|G(0) - G(1)| \leq \\ &\left(\rho_{soil} c_{soil} \Delta T_{soil,max} \Delta z_{soil} + \rho_{H_2O} W_{snow} (c_{snow} \Delta T^0_{soil,max} + L_{melt})\right) / \Delta t \end{aligned} \tag{10}$$

The superscript "0" in the snow heating term reflects the fact that snow temperatures must not exceed the melting temperature. In this approach the latent heat of fusion should of course only be considered for events when the overall energy budget of the surface layer indicates a heating and the energy required for snow melting would therefore contribute to the thermal inertia of the uppermost soil layer and moderate the layer temperature tendency. A snow layer of 10 cm would typically have a heat capacity which is larger than the corresponding value of the uppermost soil layer and the energy required to melt such an amount of snow is even larger, provided the temperature increments are not excessively large. However, for simplicity, we will omit the snow contribution in the following. These effects may simply be added in the final form of the derived equations.

The flux at the upper boundary G(0) can be decomposed in the individual contributions from sensible heat flux J_s, latent heat flux J_q, net solar F_s and net thermal radiative flux F_t. Using this decomposition, we obtain:

$$\begin{aligned} &|J_s + J_q + F_s + F_t - G(1)| \leq \\ &\quad \left(\rho_{soil} c_{soil} \Delta T_{soil,max} \Delta z_{soil} + \rho_{H_2O} W_{snow} (c_{snow} \Delta T^0_{soil,max} + L_{melt})\right) / \Delta t \end{aligned} \tag{11}$$

This equation poses an upper limit on the total flux divergence for the uppermost soil layer. Since radiative fluxes are computed independently and the soil heat flux at the lower boundary of the layer is generally small compared to the other contributions, we will try to comply with the imposed limitation through an adjustment of the sensible (and latent) heat flux. As the sensible heat flux is computed from the relation:

$$J_s = C_D |\vec{u}| \rho_a c_a \Delta T_{as} \tag{12}$$

where ΔT_{as} represents the temperature difference between atmosphere and the earths surface, $|\vec{u}|$ the near surface wind speed and C_D the dimensionless transfer coefficient for heat. The atmospheric heat capacity has a typical value of $\rho_a c_a \approx 1000 J/(m^3 K)$.

A similar equation holds for the latent heat flux, i.e.

$$J_q = C_D |\vec{u}| \rho_a L_v \Delta q_{as} \tag{13}$$

with latent heat of condensation and moisture difference between surface and atmosphere as relevant properties.

Substitution of the turbulent flux equations (12) and (13) into (11), gives:

$$\begin{aligned} &|C_D |\vec{u}| \rho_a (c_a \Delta T_{as} + L_v \Delta q_{as}) + F_s + F_t - G(1)| \leq \\ &\quad \left(\rho_{soil} c_{soil} \Delta T_{soil,max} \Delta z_{soil} + \rho_{H_2O} W_{snow} (c_{snow} \Delta T^0_{soil,max} + L_{melt})\right) / \Delta t \end{aligned} \tag{14}$$

As all other properties are either fixed or can not be changed without major complications, we will attempt to comply with the soil temperature tendency limitation through a constraint to the surface-atmosphere transfer coefficient. In order to isolate the transfer coefficient in (14), we must now introduce a distinction between heating and cooling situations for the topmost soil layer.

Let us first consider a heating of the soil, i.e. the sum of all contributions on the left hand side of (14) is positive even before taking the absolute value. In this case, we may rewrite (14) as:

$$\begin{aligned} C_D |\vec{u}| \rho_a (c_a \Delta T_{as} + L_v \Delta q_{as}) \leq \\ \left(\rho_{soil} c_{soil} \Delta T_{soil,max} \Delta z_{soil} + \rho_{H_2O} W_{snow} (c_{snow} \Delta T^0_{soil,max} + L_{melt})\right) / \Delta t \\ - F_s - F_t + G(1) \end{aligned} \tag{15}$$

Despite the supposition of an overall heating, the energy transfer by turbulent fluxes may in certain situations be directed from the soil to the atmosphere. In such situations a reduction of the turbulent transfer coefficients would be counterproductive to our intention of limiting the heating of the first soil layer. In these cases we will therefore retain the original unlimited transfer coefficient. If turbulent fluxes would provide a positive contribution to the energy budget of the soil and thereby enhance the overall heating in situations when atmosphere and soil are not in balance (e.g. after the data assimilation step) a limitation of the transfer coefficient can alleviate the problem. In this situation, we may solve (15) for C_D to obtain the following constraint for the transfer coefficient:

$$\begin{aligned} C_D \leq \{ \left(\rho_{soil} c_{soil} \Delta T_{soil,max} \Delta z_{soil} + \rho_{H_2O} W_{snow} (c_{snow} \Delta T^0_{soil,max} + L_{melt}) \right) / \Delta t \\ - F_s - F_t + G(1) \} \; / \; \{ |\vec{u}| \rho_a (c_a \Delta T_{as} + L_v \Delta q_{as}) \} \end{aligned} \tag{16}$$

The physical meaning of (16) is obvious. Compared to the threshold soil temperature tendency the remaining possible contributions by turbulent fluxes to the heating of the first soil layer is diminished by the potential contributions of radiative fluxes at the surface and the internal heat flux between soil layer 1 and 2. In the presence of snow a (substantial) part of the energy gain may be used for the heating and/or melting of the snow layer, thereby allowing an overall larger total energy input.

Let us now consider a cooling of the soil, i.e. the sum of all contributions on the left hand side of (14) is negative before taking the absolute value. In this case, we may rewrite the equation:

$$\begin{aligned} C_D |\vec{u}| \rho_a (c_a \Delta T_{as} + L_v \Delta q_{as}) + F_s + F_t - G(1) \geq \\ -(\rho_{soil} c_{soil} \Delta T_{soil,max} \Delta z_{soil} + \rho_{H_2O} W_{snow} c_{snow} \Delta T^0_{soil,max}) / \Delta t \end{aligned} \tag{17}$$

leading to:

$$\begin{aligned} C_D |\vec{u}| \rho_a (c_a \Delta T_{as} + L_v \Delta q_{as}) \geq \\ -(\rho_{soil} c_{soil} \Delta T_{soil,max} \Delta z_{soil} + \rho_{H_2O} W_{snow} c_{snow} \Delta T^0_{soil,max}) / \Delta t - F_s - F_t + G(1) \end{aligned} \tag{18}$$

Note that the snow melting term has vanished since no melting will take place, if the overall forcing is negative. A limitation of the transfer coefficient in this situation can only alleviate the temperature tendency problem of the first soil layer, if the turbulent fluxes at the surface would contribute to an energy loss. Solving for the transfer coefficient, we obtain:

$$\begin{aligned} C_D \leq \{ (-\rho_{soil} c_{soil} \Delta T_{soil,max} \Delta z_{soil} + \rho_{H_2O} W_{snow} c_{snow} \Delta T^0_{soil,max}) / \Delta t \\ - F_s - F_t + G(1) \} \; / \; \{ |\vec{u}| \rho_a (c_a \Delta T_{as} + L_v \Delta q_{as}) \} \end{aligned} \tag{19}$$

Note the reversal from $\geq$ to $\leq$ when going from (18) to (19) due to the division by a negative quantity. In the absence of other contributions (e.g. from radiative fluxes) the energy loss through turbulent fluxes from the earths surface to the atmosphere is simply constrained to keep the cooling of the first soil layer below the specified threshold value. Positive contributions to the energy balance of the soil layer (e.g. by solar radiation or an upward heat flux within the soil) imply a larger potential for an energy loss through turbulence without violation of the imposed threshold.

2.5.2 Final remarks

The above derivation of a threshold equation for the transfer coefficient does not consider that the heat conduction equation is solved implicitly in the soil scheme. However, the upper limit for the temperature increment within one time step has to be chosen rather arbitrarily anyway. And the whole mechanism is only intended for a "soft" relaxation towards a more balanced atmospheric and soil structure in hopefully rare cases of "unphysical" changes of individual state variables or forcing components. In situations were a limitation of the transfer coefficient were counterproductive, the temporal tendency of the uppermost soil layer remains unchanged. If such a situation would lead to an unstable behaviour of the soil scheme, one would either have to reduce the model time step or extend the flux limitation approach to other forcing terms like the surface radiative fluxes.

3 Pre-operational and operational use in LME

In January 2005 the pre-operational test-suite of LME was initiated using the multi-layer soil model. Because at this time GME had been running pre-operationally and operationally for more than one year, temperatures and water content values in the LME-soil could be initialised by interpolation of the respective GME-fields. Therefore, the initial values could be regarded as being fairly adjusted to the model climate. No long spin-up period had to be anticipated. The soil moisture assimilation scheme was transferred from LM to LME with some adjustment because of the different layer structure. On September 28, 2005, LME replaced LM as the operational limited area model. Since the start in January no serious problem was noted in the LME soil model.
Most of the changes made during the first year of operational GME-runs with the new soil model were implemented step by step also in LME. The large negative bias of near surface temperatures observed for the GME in March 2005 was reduced in the LME by a provisional - and in fact not correct - method to convert snow heights to snow water equivalent in the LME-analysis. Purely by chance this method considerably reduced the problem. On January 05, 2006, the time-dependent treatment of snow density became operational in LME.
LME seems not to be prone to the problem with the small amplitude waves in surface temperatures as it uses a different formulation of the surface layer processes. Although no problems in the interaction with the snow analysis were noted, the respective method of GME was copied into LME.

4 Verification of soil temperature prediction over Germany

A soil model with a large active depth used operationally obviously needs to be validated in detail. However, observations of the prognostic soil variables at different depths are not available over the whole LME domain. Fortunately, all synoptic stations over Germany regularly report soil temperatures in different depths (2 cm, 5 cm, 10 cm, 20 cm, 50 cm, and 100 cm). This allows a direct comparison of observed/simulated temperatures in depths of 5/6 cm, 20/18 cm, and 50/54 cm. Figures 2 through 7 show observed and simulated temperatures in these three pairs of depths. As to be anticipated in early autumn, temperatures increase with increasing depth both in the observations and in the model.
Unfortunately it is difficult to obtain realistic area mean values. In the case of the observations they can only be estimated by taking the arithmetic average of the values reported. The respective values of the model simulations, computed by the plot-software, are biased by the

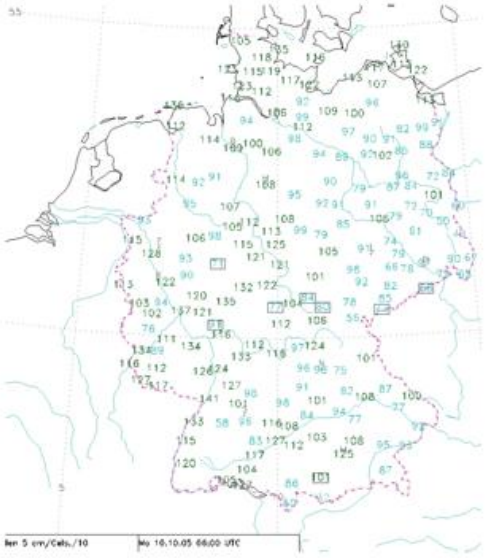

Figure 2:
Distribution of observed soil temperature $[0.1^0C]$ at 5 cm depth, 10 October 2005, 06 UTC.

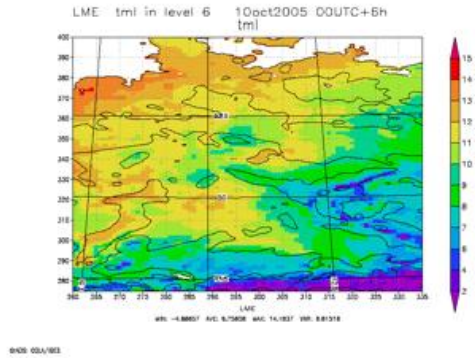

Figure 3:
Distribution of predicted soil temperature $[^0C]$ at 6 cm depth, 10 October 2005, 06 UTC.

inclusion of some part of the Alps with very low temperatures. Only very few observations are representative of higher regions, whereas the model simulations show comparably large areas with rather low temperatures because of comparably high values of the orography. Taking these effects into account, the area mean values seem to be in fairly good agreement between observation and simulation, but there seems to be some small warm bias in the model. The Upper Rhine Valley is correctly simulated as the warmest region in Germany. Although the eastern parts of northern Germany are simulated colder than the western parts, the difference is not as pronounced as in the observations. In contrast to this, some temperatures at the mountain peaks of the Thuringian Forest and of the Ore Mountains are colder in the simulations than in the observations.

5 Long-term diagnostics for LME and GME

The long-term behaviour of a soil model like the present has to be diagnosed carefully. Slow drifts might occur, especially for soil water content. A potential risk of a systematic drift in the soil temperatures is alleviated through the existence of the climate layer as a lower boundary condition. However, any systematic drift of temperatures or water content in the soil would have an impact on near surface temperatures. It is therefore mandatory to monitor the long term evolution of the soil variables in the model. For this purpose some statistical properties of the soil variables are checked on a regular basis. This monitoring is applied for layers below 0.09 m only. The rather thin three uppermost layers are excluded, as they immediately react to the atmospheric forcing. They are not characteristic of the long-term behaviour of the soil model.

5.1 Soil temperature

For the whole LME-area Table 1 shows the minimum (Min), the area averaged (Ave), and the maximum (Max) values of temperature for all soil model levels included in the diagnostic

Table 1: Minimum value (Min), area-mean (Ave), and maximum value (Max) of LME soil temperatures (^0C) in different levels of the soil model, 15 Feb 2005 - 01 Feb 2006

depth	**0.18 m**			**0.54 m**			**1.62 m**			**4.86 m**		
	Min	**Ave**	**Max**	**Min**	**Ave**	**Max**	**Min**	**Ave**	**Max**	**Min**	**Ave**	**Max**
2005												
15 Feb	-15.55	0.81	19.12	-13.25	2.30	18.46	-10.25	5.16	22.57	-11.46	9.06	29.31
15 Mar	-13.35	2.75	23.08	-12.69	3.25	24.05	-10.48	5.09	23.78	-11.46	9.05	29.15
15 Apr	-11.26	7.93	28.45	-11.51	6.94	29.75	-10.68	6.26	25.96	-11.46	9.05	29.15
15 May	-7.65	12.35	33.89	-8.27	10.94	33.54	-8.57	7.18	27.60	-14.87	8.08	24.72
15 Jun	-6.06	16.08	37.77	-6.34	14.94	36.87	-7.11	10.07	32.60	-14.87	8.09	24.80
15 Jul	-5.01	19.69	40.52	-5.27	18.03	40.79	-6.39	12.25	35.82	-14.87	8.14	26.68
15 Aug	-4.83	19.07	38.43	-3.73	18.55	40.94	-5.26	13.91	37.85	-14.88	8.29	28.61
01 Sep	-4.45	17.45	38.11	-4.50	17.64	39.47	-5.24	14.10	37.59	-14.87	8.33	29.67
11 Sep	-4.64	16.45	37.26	-4.89	16.06	38.11	-4.99	14.06	36.81	-14.87	8.33	30.11
21 Sep	-5.98	13.97	35.46	-5.06	15.25	37.12	-5.06	13.87	36.11	-14.87	8.33	30.11
01 Oct	-6.79	13.68	31.33	-6.46	14.65	33.75	-5.62	13.50	34.91	-14.87	8.33	30.11
11 Oct	-11.68	11.98	32.16	-6.72	13.28	34.16	-6.00	13.04	33.70	-14.87	8.33	30.11
21 Oct	-12.36	8.79	30.75	-8.31	11.14	31.61	-6.35	12.44	32.76	-14.87	8.33	30.11
01 Nov	-12.42	7.66	26.98	-10.37	9.75	28.64	-6.87	11.64	31.31	-14.87	8.33	30.11
11 Nov	-15.92	6.59	22.32	-10.86	8.63	26.37	-7.22	10.86	29.99	-14.87	8.33	30.10
21 Nov	-17.71	4.57	22.74	-13.36	6.78	24.04	-7.57	9.99	27.94	-14.87	8.33	29.99
01 Dec	-14.07	4.14	23.90	-13.03	5.68	25.50	-8.82	9.01	26.58	-14.87	8.33	29.36
11 Dec	-14.10	2.86	23.27	-12.00	5.12	25.31	-9.40	8.24	26.11	-14.87	8.33	28.73
21 Dec	-13.35	1,95	19.87	-11.77	3.95	22.56	-9.46	7.48	25.47	-14.87	8.32	28.11
2006												
01 Jan	-13.38	2.05	19.76	-13.11	3.37	20.78	-10.13	6.71	24.25	-14.87	8.31	27.42
11 Jan	-13.57	0.88	17.65	-11.61	2.84	21.19	-10.23	6.13	23.72	-14.87	8.27	26.99
21 Jan	-21.32	-0.93	17.75	-12.80	2.05	18.82	-9.86	5.57	22.95	-14.87	8.24	26.47
01 Feb	-14.79	-0.17	17.63	-10.96	1.45	19.61	-9.53	5.05	22.67	-14.87	8.21	26.04
11 Feb	-14.86	0.05	17.96	-10.91	1.47	19.76	-9.40	4.75	22.07	-14.87	8.19	26.03
21 Feb	-11.26	1.45	19.49	-10.29	2.22	20.34	-9.39	4.62	21.86	-14.87	8.18	26.03
01 Mar	-10.77	1.63	24.65	-10.23	2.57	23.60	-9.40	4.57	21.98	-14.87	8.14	26.03

Table 2: Area-mean (Ave) and maximum (Max) values of LME soil water content (vol %) in different layers of the soil model, 15 Feb 2005 - 11 Apr 2006, whole model area

depth	**0.09-0.27 m**		**0.27-0.81 m**		**0.81-2.43 m**	
	Ave	**Max**	**Ave**	**Max**	**Ave**	**Max**
2005						
15 Feb	26.87	82.13	22.42	80.02	24.39	68.62
15 Mar	27.27	84.18	22.84	76.72	24.34	69.67
15 Apr	24.15	85.46	23.39	77.02	24.27	70.60
15 May	22.32	82.59	22.88	85.40	24.50	72.49
15 Jun	21.84	82.86	22.17	80.45	24.63	74.01
15 Jul	20.23	85.46	20.29	80.66	24.65	74.69
15 Aug	21.27	85.91	19.30	80.50	24.57	75.54
01 Sep	19.68	82.93	18.20	78.61	24.52	75.71
11 Sep	19.66	82.17	18.04	78.30	24.47	75.69
21 Sep	21.18	81.99	18.85	78.57	24.43	75.64
01 Oct	20.00	81.97	18.46	78.72	24.40	75.61
11 Oct	19.46	81.91	18.16	85.05	24.37	75.66
21 Oct	21.45	82.02	18.61	79.07	24.34	75.76
01 Nov	22.15	82.11	18.77	79.31	24.31	75.99
11 Nov	21.77	82.25	18.50	80.05	24.31	76.31
21 Nov	23.18	82.22	18.76	80.53	24.30	76.68
01 Dec	24.20	82.60	19.52	79.53	24.30	76.95
11 Dec	24.02	82.61	19.94	78.97	24.36	77.11
21 Dec	23.54	85.61	19.89	79.51	24.42	77.26
2006						
01 Jan	23.65	86.24	19.79	79.45	24.45	77.47
11 Jan	23.39	85.83	19.88	78.54	24.48	77.56
21 Jan	23.80	85.47	19.97	78.75	24.49	77.56
01 Feb	24.24	86.12	20.33	79.09	24.49	77.60
11 Feb	24.33	86.21	20.93	78.64	24.49	77.67
21 Feb	24.85	85.84	21.35	79.08	24.50	77.75
01 Mar	25.09	85.52	21.74	78.75	24.54	77.83
11 Mar	25.04	85.51	21.83	79.07	24.58	77.81
21 Mar	24.46	85.37	21.89	79.01	24.65	77.70
01 Apr	24.22	85.29	21.72	79.11	24.73	77.83
11 Apr	24.51	85.34	22.31	79.82	24.79	77.65

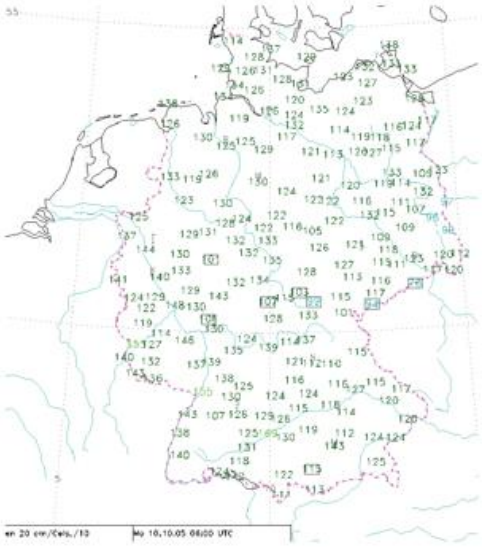

Figure 4:
Distribution of observed soil temperature $[0.1^0C]$ at 20 cm depth, 10 October 2005, 06 UTC.

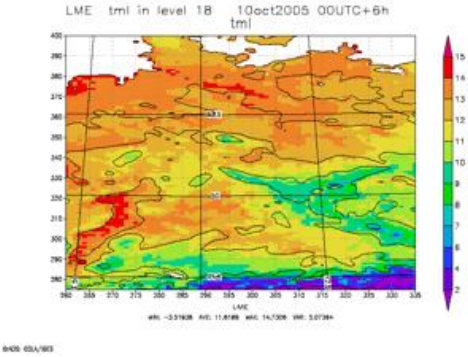

Figure 5:
Distribution of predicted soil temperature $[^0C]$ at 18 cm depth, 10 October 2005, 06 UTC.

evaluation since the start of the pre-operational LME runs in 2005. The respective values for the climatological boundary condition are: Min -11.74 ^0C, Ave 9.21 ^0C and Max 29.62 ^0C, being constant in time. The downward propagation of the annual temperature wave is clearly visible. The phase is in accord with the analytical solution of the heat conduction equation. Also, the decrease of temperature variations with increasing depth shows up in the results. In general the results appear to be realistic. There seems to be a slight discontinuity from April to May. The reason for this is a new start of LME on May 09. This was required by a new data-set of external parameters. After one year of simulation the temperatures are rather close to the initial values on 15 February, 2005. There is only a small decrease in average temperatures by less than 1 K, whereas the minimum values are slightly warmer. No uniform change is present in the maximum values. In general these results confirm the long-term stability of the soil model with respect to temperature.

5.2 Soil water content

Results for the behaviour of soil water content in LME are shown in Table 2. In the layer 0.09-0.27 m the maximum occurs in March after the snow melting in most of the model-area is finished. This high water content slowly penetrates to deeper layers. The maximum occurs in April in the layer 0.27-0.81 m and as late as August in the layer 0.81-2.43 m. Also the drying in summer is obvious, the minimum is simulated in October and November. For the whole LME-area the minimum value of soil water content is always zero because of the presence of grid-points with soil type ice or rock. For these soil types hydrological processes are not simulated and a water content of zero is prescribed. Therefore minimum values are not shown in this table. In the layers from 0.27 to 2.43 m a small decrease in average soil water content is observed. This could be a result of unsuitable initial conditions. But other data confirm a tendency of the soil model to decrease soil water content at least in part of the model area. The statistics are also available for some small regions, namely Iceland, Lapland, the Alps, and Asia Minor. Whereas for Iceland an increase in soil moisture is simulated, for the Alps a loss of 25% of the initial value is simulated for the layers from 0.27

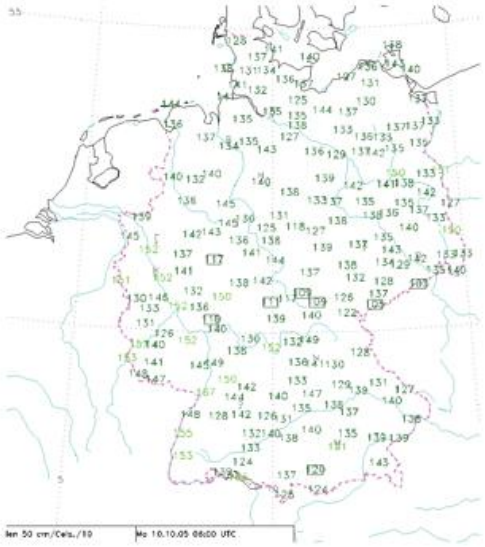

Figure 6:
Distribution of observed soil temperature $[0.1^0C]$ at 50 cm depth, 10 October 2005, 06 UTC.

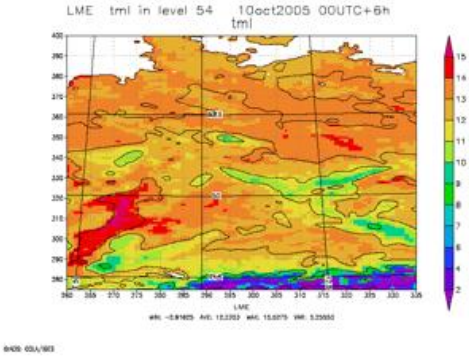

Figure 7:
Distribution of predicted soil temperature $[^0C]$ at 54 cm depth, 10 October 2005, 06 UTC.

to 2.43 m. A small decline in soil water content is also simulated for Lapland and for Asia Minor.

At the German Weather Service soil water content is measured on a regular basis in the area of the observatory Lindenberg (federal state of Brandenburg). For the year 2005 the results of the pre-operational and operational LME-runs are compared to direct measurements and to simulations performed with the model system AMBAV of the department for agricultural meteorology. AMBAV includes the very high resolution model AMBETI (Braden, 1995), which in AMBAV is driven by observations. The results of AMBAV-simulations can be used as surrogates for soil moisture measurements. Figure 8 shows a comparison of LME-forecast (6 to 30 hour forecasts for each day are combined to one quasi-annual result), direct measurements and AMBAV-results for the layer 9 to 27 cm. Taking into account for the limited comparability of direct soil water content measurements and model simulations for a rather large area (7 x 7 km^2), the results agree fairly well until the end of the second quarter of the year. But in July and August there is excessive drying in the LME-results. This effect is only partly compensated in September. In December the moisture values are much lower (roughly 50 %) than in January.

It must be noted that at DWD the operational LME is run including a soil moisture assimilation scheme (SMA). The SMA reacts on errors in the predicted 2m-temperatures, changing soil water content in order to minimize the error. The SMA partly counteracts changes of soil water content due to forcing by precipitation, evapotranspiration and runoff. During the pre-operational phase in 2005, the SMA-increments of soil water content in LME were compared with the respective changes in the operational LM (at the time with the old two-layer soil model). The average values for the LM-area turned out to be very similar in both models. This indicates that on average the multi-layer model and the old two layer model react in a nearly identical manner on the forcing of soil water content.

In Table 3 the soil water content values for GME are presented. Only the values determined for the LME-area are shown, in order to allow a comparison with the values for LME in Table 2. Obviously there is a much stronger decrease in soil water content in GME compared to LME in the upper layers during summer. This is consistent with the effect of the SMA, which in summer on average moistens the soil. But at the end of the one year period shown

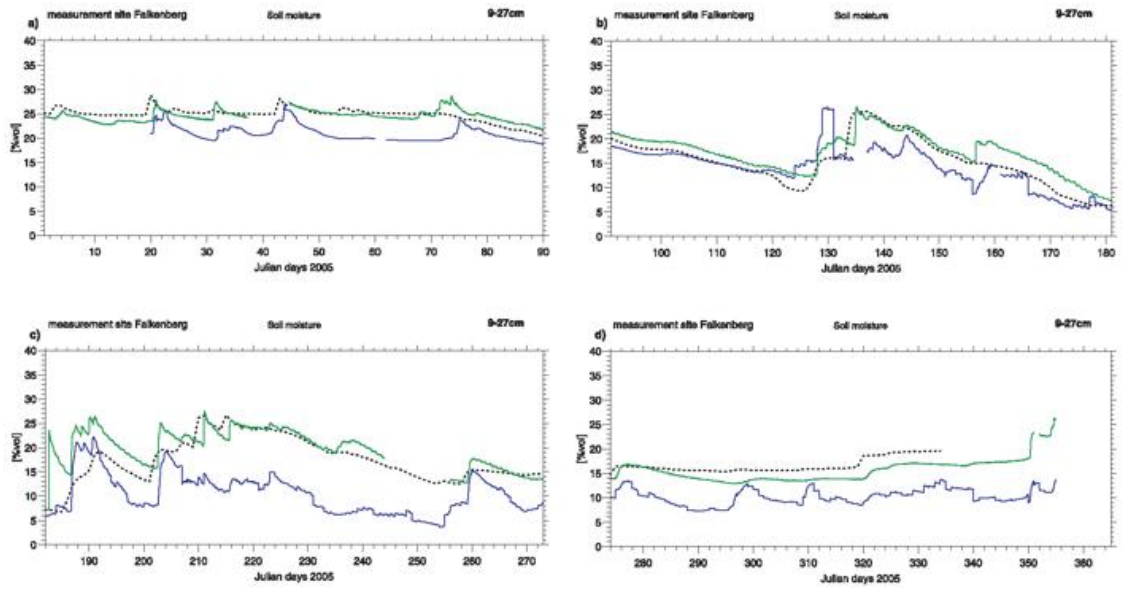

Figure 8:
Soil moisture (Vol %) in the layer 9 - 27 cm for the year 2005. Green: direct measurements, dotted: AMBAV-simulations, blue: LME-forecasts. a) January -March, b) April - June, c) July - September, d) October - December. See text for details.

in Table 3 the vaues are quite similar to the values in April 2005.

6 Changes after the operational implementation

The operational results of GME and LME with the multi-layer soil model revealed some problems. This resulted in changes of the soil model, which are described in this section.

6.1 Dependence of snow albedo on time and on forest cover

The first operational version of the multi-layer soil model used a constant snow albedo for solar radiation of 70%. Forest cover was not used to decrease the mean solar albedo in the case of existing snow decks. GME-results - especially in North America - revealed a strong negative temperature bias in spring. This could well be the effect of too high albedo values of old snow decks and snow cover in forested areas. This led to a reformulation of snow albedo. A snow-age indicator f_{snow} is introduced, being 1 for 'fresh' snow and 0 for 'old' snow. The albedo of snow is determined by

$$\alpha_{snow} = \alpha_{snow,max} \cdot f_{snow} + \alpha_{snow,min} \cdot (1 - f_{snow}), \tag{20}$$

where $\alpha_{snow,max} = 0.7$ and $\alpha_{snow,min} = 0.4$. The snow-age indicator is updated every time-step. One effect is a slow ageing term $\Delta t/\tau_\alpha$ with the time-step Δt of the model and a time constant $\tau_\alpha = 28d$. The second effect is a regeneration by falling snow: RR_{snow}/RR_{norm}, where RR_{snow} is the predicted rate of snowfall, and $RR_{norm} = 5mm/d$. Then the change of f_{snow} in one time-step Δt is given by

$$\Delta f_{snow} = f_{snow}\,[RR_{snow}/RR_{norm} - \Delta t/\tau_\alpha] \tag{21}$$

Table 3: Area-mean (Ave) and maximum (Max) values of GME soil water content (vol %) in different layers of the soil model, 15 Apr 2005 - 15 Apr 2006, values are average and maximum for the LME-area

depth	**0.09-0.27 m**		**0.27-0.81 m**		**0.81-2.43 m**	
	Ave	**Max**	**Ave**	**Max**	**Ave**	**Max**
2005						
15 Apr	24.49	80.11	23.91	78.35	25.19	72.03
15 May	22.74	76.67	22.59	75.97	25.27	73.15
15 Jun	19.89	75.77	18.46	73.30	25.08	73.63
15 Jul	17.10	72.11	15.14	69.09	24.68	73.60
15 Aug	19.40	74.24	13.90	66.16	24.21	73.12
15 Sep	18.39	77.00	13.73	68.75	23.96	72.65
15 Oct	17.88	79.87	14.72	79.59	23.86	72.59
15 Nov	22.28	81.20	16.92	79.15	23.82	73.55
15 Dec	24.97	81.08	20.25	79.53	23.98	75.16
2006						
15 Jan	25.88	80.79	21.60	79.38	24.19	76.90
15 Feb	26.78	80.90	22.38	79.93	24.28	78.30
15 Mar	26.75	81.97	23.26	78.66	24.51	79.15
15 Apr	25.33	79.50	23.18	79.07	24.72	79.63

The snow-age indicator is initialised with 1.
Having determined the albedo of snow by (20), the value is reduced depending on forest cover. Although separate values are available for evergreen and for deciduous forests, respectively, at present we only use the total fractional forest cover σ_{forest} to compute the final snow albedo α_{sf} by

$$\alpha_{sf} = \alpha_{snow} \cdot (1 - \sigma_{forest}) + \alpha_{forest} \cdot \sigma_{forest}, \tag{22}$$

with $\alpha_{forest} = 0.2$.

6.2 Increase of infiltration at the expense of surface runoff

The indications given in the chapter on the long-term diagnostics for LME and GME on a possible drying of the soil led to some investigation of likely reasons for this behaviour. It turned out that the extremely low value of 10^{-6} m prescribed as the maximum value of the water content in the interception store had an unwanted effect on infiltration. As nearly no rain could be stored in the interception store, being available for later infiltration, nearly all rain was converted to runoff (see the paragraph on 'Interception store, Infiltration of Rain and Runoff from Interception Store' in the extended LM-documentation (Doms et al., 2005)). The parameter α tended to be 1, therefore in $I_{rain} = (1 - \alpha)P_r$ no rain is converted to infiltration. This situation was improved by artificially prescribing $\alpha = 0$. In GME a remarkable effect occurred, especially in the areas of high convective precipitation in the tropics. In LME only a very small effect could be noted, because the soil moisture assimilation masked most of the possible impact.

7 Suggested future work

There are especially three areas for future model improvement:

- The drying of the soil deserves further attention. A flux equal to zero at the lower

boundary of the hydrologically active layers should be tested. This could especially be advantageous in areas with long periods of snow cover. As long as the deeper soil layers are not completely frozen, the gravitational flux will reduce the water content. This might be the reason for extremely low soil moisture values in the Alps.

- A tile approach, which distinguishes between - at least - snow-covered and snow-free parts of a grid element will be helpful for temperature prediction in the case of melting snow. Presently the soil surface temperature sticks to 0^oC as long as some part of the grid element is snow-covered. This leads to much too cold 2m-temperatures in situations with melting snow. In reality the soil surface temperature in the snow-free areas of the grid element can be considerably warmer than 0^oC.

- With a much larger effort the implementation of a multi-layer snow module should be considered. Such a model can deal with the layered structure of old snow decks and with the downward transport of water (rain or melted snow) through the snow. Also, the problem of snow density can be dealt with in a much more consistent manner.

8 Summary

A multi-layer soil model was implemented and tested in GME and LME. As a main new feature the model includes the effect of freezing/melting of soil water/ ice. Thorough testing in the global model GME preceded the pre-operational (since January 2005) and operational (since September 28, 2005) use in LME. The soil moisture assimilation scheme of LM was adjusted to the new layer structure and used in the pre-operational LME-runs since May 2005. A lot of minor and also some major bugs in the model were detected and corrected through the (pre)operational runs. Additionally, some improvements have been introduced in the code in the years 2005 and 2006. The long-term behaviour of soil water content still deserves special attention.

9 Acknowledgement

A lot of technical problems in the interplay of analysis, interpolation from GME to LME and operational LME-runs had to be solved with the help of M. Buchhold, Th. Hanisch and U. Schättler. M. Arpagaus and his colleagues at Meteoswiss used the multi-layer soil model in parallel runs and provided a lot of input for the improvement of the model. P. Meyring performed the diagnostic evaluation of the model results and assisted in solving problems with different graphic formats.

10 References

Boone, A., F. Habets, and J. Noilhan, 2001: The Rhône-AGGregation Experiment, GEWEX News, WCRP, 11(3), 3-5.

Braden, H., 1995: The model AMBETI. A detailed description of a soil-plant-atmosphere model. Berichte des Deutschen Wetterdienstes, Nr. 195, 117 pp.

Doms, G., J. Förstner, E. Heise, H.-J. Herzog, M. Raschendorfer, R. Schrodin, Th. Reinhardt, and G. Vogel, 2005: A description of the Nonhydrostatic Regional Model LM, Part II: Physical parameterization. See: www.cosmo-model.org

Heise, E., M. Lange, B. Ritter, and R. Schrodin, 2003: Improvement and Validation of the Multi-Layer Soil Model. COSMO Newsletter No. 3, February 2003, 198-203.

Schrodin, E., and E. Heise, 2002: A New Multi-Layer Soil Model. COSMO Newsletter No. 2, February 2002,149-151

List of COSMO Newsletters and Technical Reports

(available for download from the COSMO Website: www.cosmo-model.org)

COSMO Newsletters

No. 1: February 2001.

No. 2: February 2002.

No. 3: February 2003.

No. 4: February 2004.

No. 5: April 2005.

No. 6: July 2006; Proceedings from the COSMO General Meeting 2005.

COSMO Technical Reports

No. 1: Dmitrii Mironov and Matthias Raschendorfer (2001):
Evaluation of Empirical Parameters of the New LM Surface-Layer Parameterization Scheme. Results from Numerical Experiments Including the Soil Moisture Analysis.

No. 2: Reinhold Schrodin and Erdmann Heise (2001):
The Multi-Layer Version of the DWD Soil Model TERRA_LM.

No. 3: Günther Doms (2001):
A Scheme for Monotonic Numerical Diffusion in the LM.

No. 4: Hans-Joachim Herzog, Ursula Schubert, Gerd Vogel, Adelheid Fiedler and Roswitha Kirchner (2002):
LLM ¯ the High-Resolving Nonhydrostatic Simulation Model in the DWD-Project LITFASS.
Part I: Modelling Technique and Simulation Method.

No. 5: Jean-Marie Bettems (2002):
EUCOS Impact Study Using the Limited-Area Non-Hydrostatic NWP Model in Operational Use at MeteoSwiss.

No. 6: Heinz-Werner Bitzer and Jürgen Steppeler (2004):
Documentation of the Z-Coordinate Dynamical Core of LM.

No. 7: Hans-Joachim Herzog, Almut Gassmann (2005):
Lorenz- and Charney-Phillips vertical grid experimentation using a compressible nonhydrostatic toy-model relevant to the fast-mode part of the 'Lokal-Modell'

No. 8: Chiara Marsigli, Andrea Montani, Tiziana Paccagnella, Davide Sacchetti, André Walser, Marco Arpagaus, Thomas Schumann (2005):
Evaluation of the Performance of the COSMO-LEPS System

No. 9: Erdmann Heise, Bodo Ritter, Reinhold Schrodin (2006):
Operational Implementation of the Multilayer Soil Model

COSMO Technical Reports

Issues of the COSMO Technical Reports series are published by the *Consortium for Small-Scale Modelling* at non-regular intervals. COSMO is a European group for numerical weather prediction with participating meteorological services from Germany (DWD, AWGeophys), Greece (HNMS), Italy (UGM, ARPA-SMR, ARPA Piemonte) and Switzerland (MeteoSwiss). The general goal is to develop, improve and maintain a non-hydrostatic limited area modelling system to be used for both operational and research applications by the members of COSMO. This system is initially based on the Lokal-Modell (LM) of DWD with its corresponding data assimilation system.

The Technical Reports are intended

- for scientific contributions and a documentation of research activities,
- to present and discuss results obtained from the model system,
- to present and discuss verification results and interpretation methods,
- for a documentation of technical changes to the model system,
- to give an overview of new components of the model system.

The purpose of these reports is to communicate results, changes and progress related to the LM model system relatively fast within the COSMO consortium, and also to inform other NWP groups on our current research activities. In this way the discussion on a specific topic can be stimulated at an early stage. In order to publish a report very soon after the completition of the manuscript, we have decided to omit a thorough reviewing procedure and only a rough check is done by the editors and a third reviewer. We apologize for typographical and other errors or inconsistencies which may still be present.

At present, the Technical Reports are available for download from the COSMO web site (www.cosmo-model.org). If required, the member meteorological centres can produce hard-copies by their own for distribution within their service. All members of the consortium will be informed about new issues by email.

For any comments and questions, please contact the editors:

Massimo Milelli
Massimo.Milelli@arpa.piemonte.it

Ulrich Schättler
Ulrich.Schaettler@dwd.de